MULTI-NUCLEON TRANSFER REACTIONS IN $^{238}U+^{64}Ni$ USING GRAZING MODEL

A.Spătaru[1,2,4], T.Dickel[4,5], W.R.Plaß[4,5], J.S.Winfield[4], P.Constantin[1], D.L.Balabanski[1,2], D.Nichita[1,2], A.Rotaru[3], A.State[2,3]

Multi-nucleon transfer (MNT) reactions give access to heavy exotic neutron-rich nuclei which are difficult to be produced by fission or in fragmentation reactions. The $^{238}U+^{64}Ni$ MNT reactions taking place inside a gas cell, is simulated with the GRAZING code. Simulations of the release of reaction product from the target and of their slowing down in the He gas of the cell are performed with the GEANT4 software. The space charge effects induced by gas ionization are studied with the SIMION program. The implications for an experimental program using such a setup are discussed.

Keywords: multi-nucleon transfer reactions, quasi-fission, cryogenic stopping cell

1. Introduction

Experimental studies of neutron-rich exotic nuclei along the r-process path aim at improving our understanding in fields like nuclear structure, nuclear equation of state and nuclear astrophysics. The usual techniques to produce such nuclei, are fission or fragmentation [1].

Reaching the heavy nuclei with $Z > 65$ in these reactions becomes difficult due to the steeply declining production cross-sections. The cross-section [2] of multi-nucleon transfer (MNT) reactions, where several nucleons are exchanged between heavy ions colliding at energies slightly above their Coulomb

[1]Extreme Light Infrastructure Nuclear Physics, Horia Hulubei National Institute for R&D in Physics and Nuclear Engineering, 30 Reactorului Str., 077125 Bucharest Magurele,Romania, e-mail: anamaria.spataru@eli-np.ro

[2]Doctoral School in Engineering and Applications of Lasers and Accelerators, University Polytechnica of Bucharest, Romania

[3]Horia Hulubei National Institute for R&D in Physics and Nuclear Engineering, 30 Reactorului Str., 077125 Bucharest Magurele, Romania

[4]GSI Helmholtz Centre for Heavy Ion Research GmbH - Planckstrasse 1, 64291 Darmstadt,Germany

[5] II. Physikalisches Institut,Justus-Liebig-Universitat Giessen,35392 Giessen, Germany

barrier and reaction products are emitted around the grazing angle, have a significantly slower decrease. In the last years this has led to an increased interest in using such reactions for the production of heavy neutron-rich nuclei.

In addition to the increased cross-section around the grazing angle, a significant fraction of the reaction products are emitted away from the forward direction. As a result, the beam can be stopped in a beam dump, placed after the target, without affecting significantly the reaction products. For a ^{238}U beam with an energy of 12 MeV/n energy and a 40 μm ^{64}Ni target, an initial estimate on the magnitude of the grazing angle of around 7 degrees is obtained with LISE++ [3]. The distribution of the energy as a function of the emission angle of the two reaction products as shown in Figure 1. There are small deviations in emission angles of the projectile-like fragments (PLFs) as compared to the large range of scattering angles of the target-like fragments (TLFs).

MNT reactions can be used at in-flight and gas ion catcher facilities. An in-flight fragment separator setup that studies MNT reactions is VAMOS at Ganil [4], a revolving arm spectometer scanning angles around the direction of the grazing angle with time-of-flight and implantation detectors. The typical disadvantage of such setups is the small angular acceptance, allowing the direct detection of the PLFs only. TLFs are measured indirectly, by their decay radiations, usually gammas, which requires knowledge about the decay scheme. Another disadvantage is the lack of a well formed radioactive ion beam (RIB) which hinders some high resolution measurements. The main advantage is the very small production to detection time, allowing the measurement of very short-lived isomers.

A gas ion catcher facility employing MNT reactions is KISS at RIKEN [5]. The main components are a stopping cell operated at room temperature, a laser system for particle ionization and a detection system. The use or argon as stopping gas gives high stopping efficiency (90%) and the laser system provides a very good accuracy for the selection of the ions of interest. On the other hand the current ensemble has also some disadvantages. The most important ones come from the use of the cell at room temperature which imply the neutralization of ions in the gas and the use of a laser system for re-ionization. This leads to the need of a new laser frequency for each element to be measured. The second disadvantage comes from the absence of electric fields for the transport of the reaction products to the cell exit nozzle which leads to large extraction times (0.5 s) [6].

This paper presents studies made with three software packages on the production, release and stopping of MNT products in a high-density gas cell with electric fields for fast extraction. The programs used are GRAZING [7], which calculates the MNT reaction cross sections, GEANT4 [8], which simulates the transport and thermalization of the products inside the target

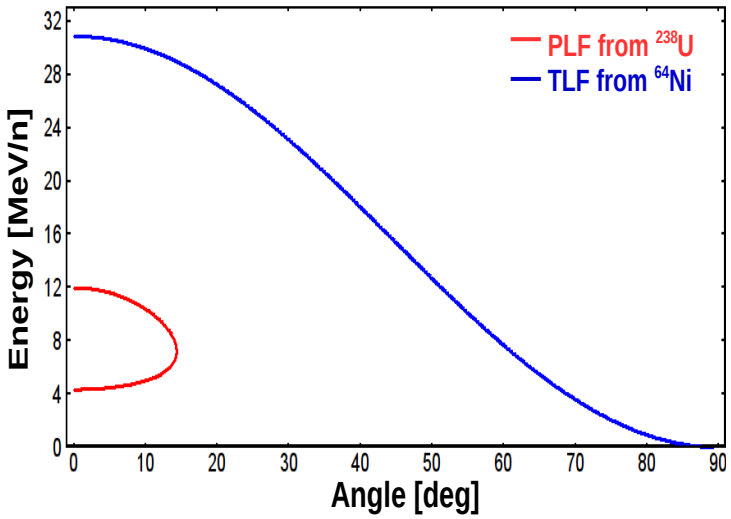

FIGURE 1. Distribution of energy as function of emission angle for projectile-like fragments (PLFs, red line) and target-like fragments (TLFs, blue line) in the $^{238}U+^{64}Ni$ reaction at 12 MeV/n.

and the gas, and SIMION [9], which simulates the space charge effect generated in the gas by ionization.

These studies are the starting point for a potential experimental program at the FRS Ion Catcher facility at GSI [10]. This facility combines gas ion catcher technique for complex manipulations and measurements of the RIBs formed in reactions induced by relativistic heavy-ion beams on various targets. These targets are placed at the beginning of the FRS. Here, the possibility to place targets inside the Cryogenic Stopping Cell (CSC) is investigated. The main components of the FRS Ion Catcher facility are the in-flight Fragment Separator (FRS), the CSC, the Radio-Frequency Quadrupole (RFQ) and a Multiple-Reflection Time-of-Flight (MR-TOF) mass spectrometer [11]. The advantages that come with the design of the CSC are an extraction time as low as 24 ms [12] which is due to the use of a DC field and a Radio-Frequency carpet to drift the ions from the stopping point to the exit nozzle. The excellent mass resolving power $m/\Delta m > 5 \cdot 10^5$ [11] of the MR-TOF allows the selection of isomerically pure RIBs [13]. The temperature of the He gas in the stopping cell is below 90 K, which keeps the gas purity at ppb levels, allowing the reaction products to reach the nozzle in 1^+ charge state. Thus, laser re-ionization is not necessary and the produced RIBs contain the full range of nuclide species produced in the reaction.

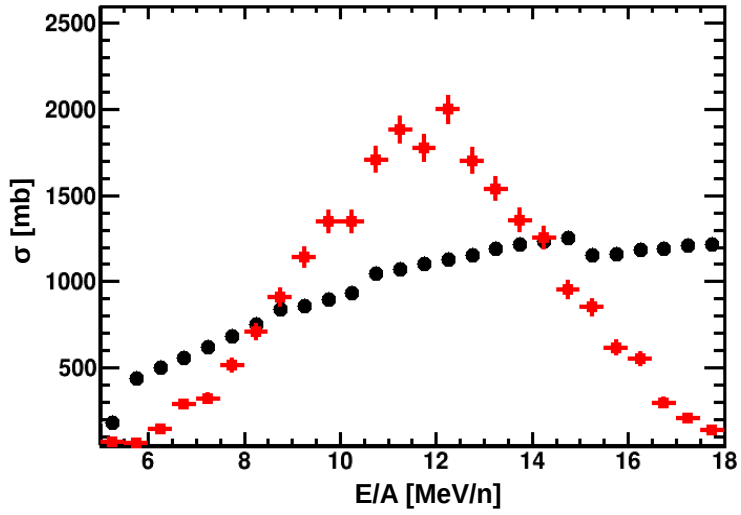

FIGURE 2. Total reaction cross section in the Grazing model after evaporation (black circles) compared to the initial beam energy profile (red squares).

2. Multi-nucleon transfer reaction and the GRAZING code

The process of multi-nucleon transfer has been studied for almost sixty years, starting with the experiments of Kaufmann and Wolfgang [14], but it is still not fully understood. An early interpretation of the process was done in Ref. [15]. It is assumed that for low energies of the incoming particle and an impact parameter smaller than that for quasi-elastic reactions, the incident particle interacts with the target by forming a deformed system with an excited neck structure. In the evolution of such systems, neutrons and protons are exchanged between the two initial particles. As the excitation energy is consumed, fragments separate without the formation of a compound nucleus.

The theoretical studies of Winther [16] for the MNT reaction in deep inelastic grazing collisions were implemented in the simulation code GRAZING. It is the main simulation tool used for such reactions using a semi-classical approach. However, nuclear deformations and fissioning of the resulting reaction products are not taken into account.

The availability at GSI of multi-GeV ^{238}U beams allows the study of nuclear reactions at energies above the Coulomb barrier of many heavy targets where the transfer of several heavy nucleons can occur.

The particular reaction chosen for this study is $^{238}U+^{64}Ni$ because it has been measured by Corradi et al. [17], and a validation of the concept can be done based on this data. The GRAZING total reaction cross-section for this reaction is shown in Figure 2 with black dots. The cross-section drops quickly below the Coulomb barrier collision energy of $B_C \approx 6$ MeV/n, which

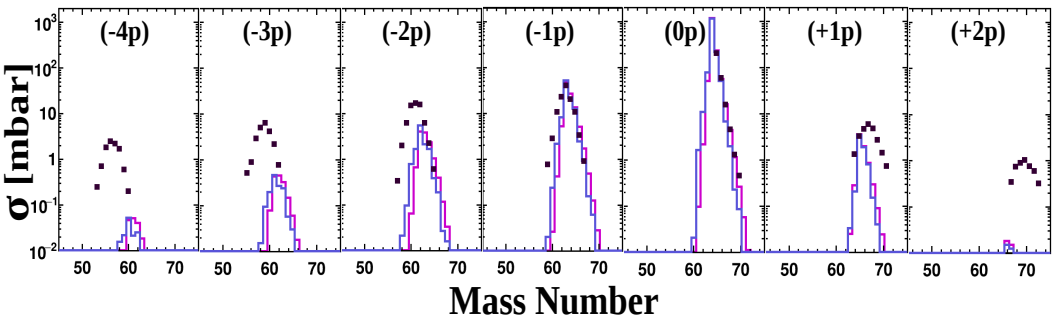

FIGURE 3. Experimental cross-sections (black squares) for the $^{64}Ni+^{238}U$ reaction at E_{lab}=390 MeV from Ref. [17] and GRAZING calculations (full lines) for the $^{238}U+^{64}Ni$ reaction at the same energy. The blue and red lines correspond to the cross-sections before and after evaporation, respectively.

suggests using a ^{238}U beam centered at 12 MeV/n and a width of 3 MeV/n. The Gaussian beam profile with these parameters is shown in Figure 2 with red dots.

The experiment and the analysis described in Ref. [17] is focused on the comparison between experimental observables and GRAZING model for the $^{64}Ni+^{238}U$ reaction at E_{lab} = 390 MeV. The setup which was used in this experiment, consisted of a time-of-flight magnetic spectrometer and a scattering chamber. The mass, charge, energy and angular distribution for the light nuclei were measured.

A comparison between the measured cross-sections in several channels from Ref. [17] and the corresponding calculations with GRAZING is shown in Figure 3. The data for proton stripping and pick-up channels in the TLF region is shown with black circles and the GRAZING cross-sections used as input for the Geant4 simulations reported in this paper are shown with full lines. The blue and red lines correspond to cross-sections before and after the evaporation of the reaction products, respectively. It should be noted that the fission channel is not included. Good agreement is demonstrated for the one or two nucleon transfer channels, but significant disagreement develops for transfers of large numbers of nucleons.

3. **Process and detector implementation in GEANT4**

The implementation of an experiment in GEANT4 typically implies the addition of three modules to the framework of this software package. The first generates the beam properties, which in our case has the simple Gaussian profile shown with red squares in Figure 2. The second module adds the specialized physics process to be studied to the queue of general physics processes

already implemented. The last module defines the geometry, materials and electromagnetic fields of the detection setup.

The $\sigma(E, Z, N)$ cross-sections in reactions considering a ^{238}U beam in the energy range E/A = 5-18 MeV/n, in steps of 0.5 MeV/n, and a ^{64}Ni target were calculated with GRAZING code. Examples of such cross-sections in the TLF region are shown in Figure 3. The total reaction cross-section

$$\sigma_R(E_0/A) = \sum_{Z,N} \sigma(E_0, Z, N)$$

shown in Figure 2 with black dots, is evaluated at the current projectile energy E_0 and is used by GEANT4 to compute the reaction mean free path and establish when and where a reaction takes place inside the target. After a reaction happens, its final state products are defined. The reaction products are generated from the normalized $\sigma(E_0, Z, N)/\sigma_R$ distributions and their kinematic parameters are derived from energy-momentum conservation. The elastic Coulomb scattering as well as other physics processes concerning nuclei, e.g. inelastic ionization and ionic energy loss, secondary electrons, e.g. standard electromagnetic processes, and photons generated in the detector are implemented by default in GEANT4.

A cylindrical gas cell with the parameters optimal for the operation of the CSC at the GSI Ion Catcher facility was implemented in GEANT4. The cell is filled with He gas at 90 K and 200 mbar, hence the gas density is 100 μg/cm^3, and a DC field of 5 kV with cylindrical symmetry was applied in the region between the target and the exit plane of the CSC.

Nuclear reactions which were studied so far at the Ion Catcher facility were generated in targets placed upstream of the CSC, at the beginning of FRS. The experiment which is studied in this work, implies a target placement inside the gas cell. An optimal stopping of the energetic reaction products favors a placement around the entrance of the CSC. However, a short-length and high-field setup, given by a placement closer to the exit wall of the CSC, reduces the space charge effect and minimizes ion drift time. The latter is achieved at a CSC length of about 25 cm, leading to DC a field of 200 V/cm, which is very effective in canceling the field induced by space charge. A compromise that considers both effects is considered.

4. **Reaction product yields and kinematics**

The first step of the simulation is finding the optimal thickness of the ^{64}Ni target for which the maximum product yield is released in the gas of CSC. The generated and released product yields, as function of the target thickness, are shown in Figure 4 with red circles and blue squares, respectively. Both yields have been normalized to a beam intensity of 10^7 ions/s. For thin targets, all the reaction products are released but the generation yield is small. For thick targets, the generation yield is large but the release efficiency is small. An intermediate target thickness of 25 μm was used initially in the calculations.

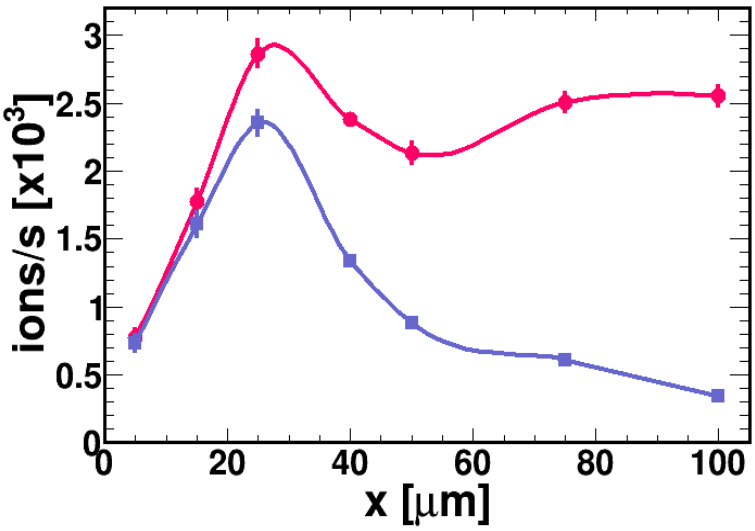

FIGURE 4. Yield of generated ions (red) compared to yield of released ions (blue) as function of the thickness of the target.

However, in this case the released products are too energetic and cannot be stopped in the gas. Thus almost all of them hit the cell walls. By increasing the thickness of the target, a lower release yield is obtained, but more efficient stopping in the gas is achieved. Finally, a target thickness of 40 μm was chosen.

At this thickness, more than 90% of the uranium beam passes through the target and needs to be stopped in order to minimize the gas ionization. A beam dump with a thickness of 3 mm and the same diameter as the target is placed 5 cm after the target and inside the gas cell. It completely stops the beam and significantly reduces the yield of electromagnetic radiation generated during the beam stopping.

The dependence of the stopped product yield on the length L of the gas cell is shown in Figure 5. While a saturation rate is reached for lengths around 60 cm, taking into account the optimal value of 25 cm for space charge and ion drift effects discussed above implies that the optimal CSC length is around 40 cm.

For an initial beam intensity of 10^7 ions/s and a target thickness of 40 μm, about $2 \cdot 10^3$ products/s are generated while 60% of PLFs and 52% of TLFs are released from the target. The distributions of the generated (black circles) and released (red circles) ions/s as a function of the energy is shown in Figure 6. While the TLFs exit the target with a broad angular distribution centered at 35°, the PLFs exhibit a narrow peak at 15° with a tail towards 0°. The beam dump cuts only the small angle tails of the MNT distributions. About 4.7% of the released PLFs and 1.9% of released TLFs are lost in the beam dump. In summary, for a CSC length of 40 cm, about 3.8% of the PLF

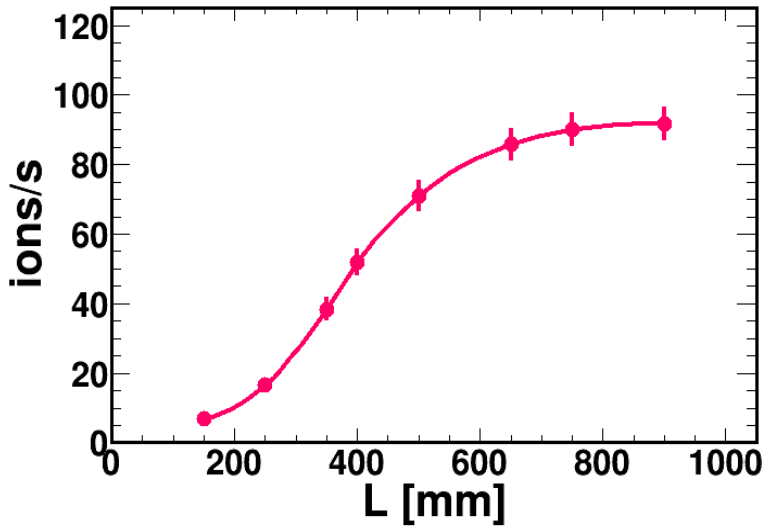

FIGURE 5. Yield of stopped ions as function of the cell length.

and the TLF are stopped in the gas of the CSC, resulting in the yields of stopped reaction products of approximately 47 PLFs/s and 6 TLFs/s.

5. Space charge effect

Helium gas ionization produces three regions of space charge in the CSC. The primary space charge region, found between the target and the beam dump, is created by the penetrating uranium beam and is strong enough to lead to the creation of a weak plasma. The secondary space charge region, found between the beam dump and the exit nozzle of the CSC, is created by the electromagnetic radiation generated by the beam during its stopping in the beam dump. The nuclear reaction space charge, spread over the entire CSC volume, is created by the reaction products during their stopping. The last two regions are characterized by low induced fields, which can only slightly alter ion trajectories and increase their drift time.

The Potential Energy Surface (PES) of the electric field generated by the DC electrodes of the CSC, as calculated by the SIMION 8.1 software, is shown in Figure 7 for the longitudinal plane (left panel) and the transversal plane (right panel).

The effect of the induced space charge on the reaction product trajectories is shown in Figure 8. The Particle-In-Cell (PIC) library of SIMION 8.1 dynamically computes the time and space dependent electric field generated by all heavy ions and He^+ ions, as they propagate and interact among themselves in the applied DC field shown in Figure 7. Note that, for clarity reasons, only a small fraction of the the He^+ ions are shown in Figure 8. Some of the reaction products can be seen deviating to the CSC outer cage due to the repulsion exerted by the primary space charge region. These heavy ions will be lost.

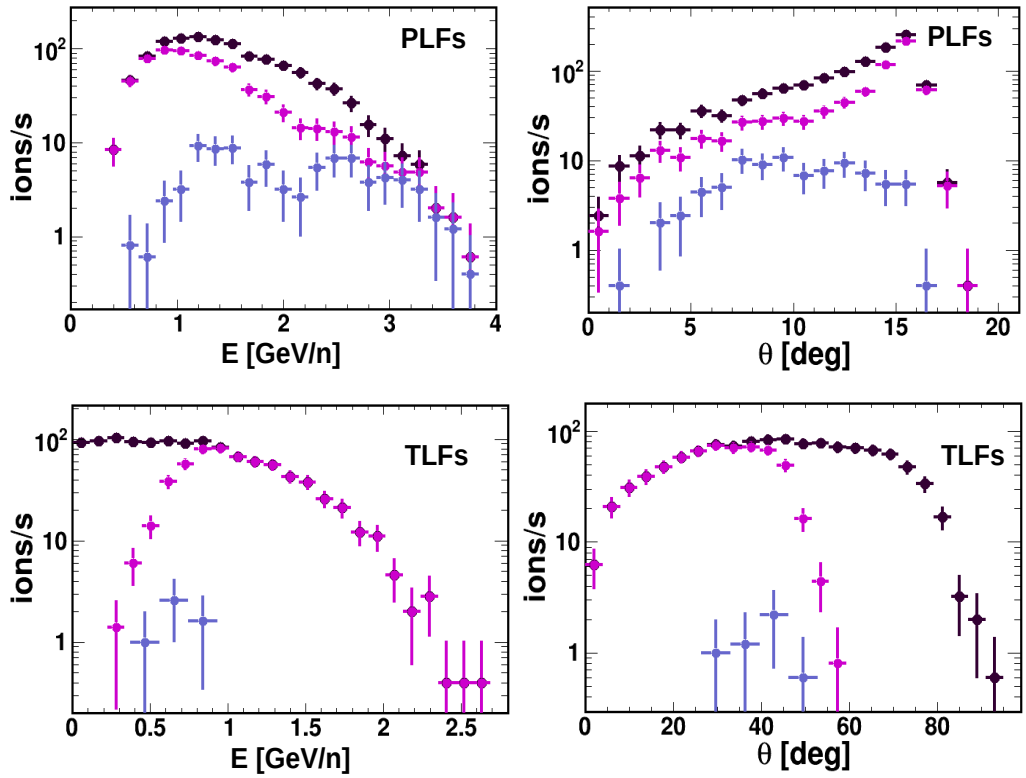

FIGURE 6. Left top and bottom panels show the PLF and TLF energy distributions. Right top and bottom panels show the PLF and TLF angular distributions. Black, red and blue circles show generated, released and stopped yields, respectively.

The large majority of the heavy ion trajectories reach the RF carpet wall on the bottom of the figure. In conclusion, no significant impact of the primary space charge region on the heavy ion extraction time and efficiency is found in these calculations.

6. Conclusions and outlook

The study, described in the present paper, aimed the optimization of a MNT experimental setup using the GRAZING model and Geant4 simulations. The considered experimental configuration consists of a 100 cm long gas-filled cryogenic stopping cell and a time-of-flight based detection system. The MNT reactions generated at about 40 cm from the CSC exit in a 40 μm ^{64}Ni target impinged by a 12 MeV/n ^{238}U beam produce stopped product yields of 47 PLFs/s and 6 TLFs/s.

Further studies of this type of reaction are necessary. The present theoretical model used, GRAZING, does not take into consideration the nuclear

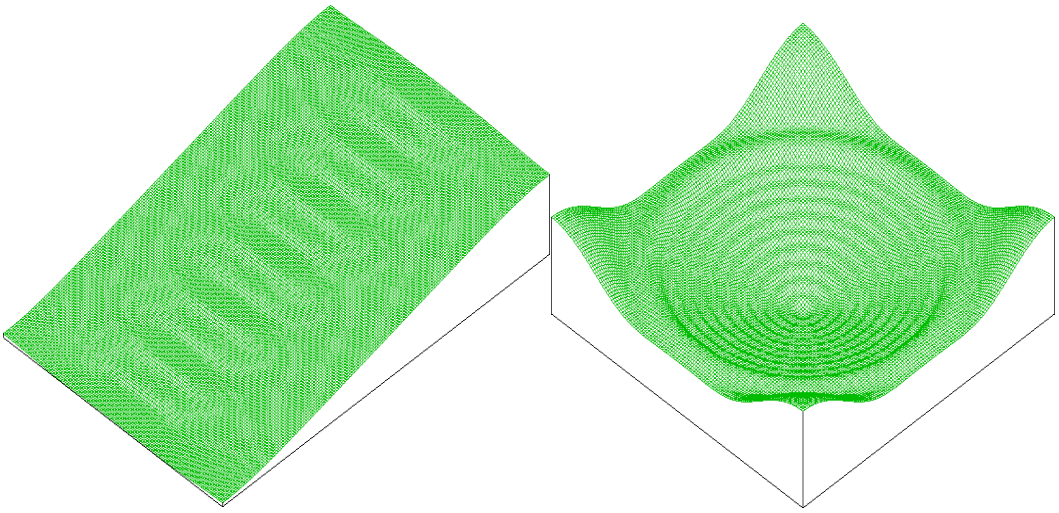

FIGURE 7. Electric PES of the CSC electrodes: longitudinal component in the left panel and transversal component in the right panel.

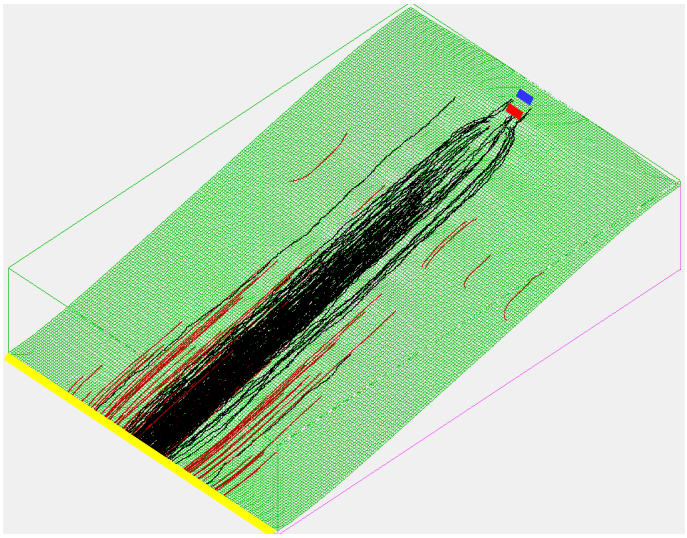

FIGURE 8. PIC simulation of the heavy (black lines) and He^+ (red lines) ion trajectories in the applied PES (green mesh) with the SIMION 8.1 sofware. The target is shown as a blue box, the beam dump as a red box and the carpet as a yellow line.

deformations of the target and projectile or the fission of the products. Also, the kinematic properties of the evaporated products is not fully implemented. New models, such as the one based on the Langevin equations in Ref. [18] offer an improved input for the simulations. Moreover, the studies can be extended to other targets that can facilitate the production of neutron-rich isotopes.

An example is the reaction $^{238}U+^{164}Dy$ that can provide information of the r-process peak and therefore would facilitate a better understanding of the formation of heavy neutron-rich isotopes during nucleosynthesis. The current FRS setup at GSI, or its future upgrade Super-FRS, can be used to generate radioactive secondary ion beams which can be used in nuclear reactions leading to very exotic nuclei.

7. Acknowledgements

This work was carried out under contract sponsored by the Ministry of Research and Innovation: PN 19 06 01 05.

REFERENCES

[1] *M. Thoennessen*, Current Status and Future Potential of Nuclide Discoveries, Rep. Prog. Phys. **76** (2013) 056301

[2] *Y.X. Watanabe et. al.*, Pathway for the Production of Neutron-Rich Isotopes around the N=126 Shell Closure, Phys. Rev. Lett. **115** (2015) 172503

[3] *O. Tarasov, D. Bazin*, Development of the program LISE: application to fusionevaporation, Nucl. Inst. Meth. B **204** (2003) 174-178

[4] *A. Vogt et al.*, Light and heavy transfer products in $^{136}Xe+^{238}U$ multinucleon transfer reactions, Phys. Rev. C **92** (2015) 112

[5] *Y. Hirayama et al.*, β-decay spectroscopy of r-process nuclei with N = 126 at KISS, Nucl. Inst. Meth. B **317** (2013) 480-483

[6] *Y. Watanabe et al.*, KEK Isotope Separation System (KISS), Nuclear Physics News, Vol. 28, No. **4**, (2018)

[7] *A. Winther*, Grazing reactions in collisions between heavy nuclei, Nucl. Physics A **572** (1994) 191-235

[8] *S. Agostinelli, et. al.*, Geant4-a simulation toolkit, Nucl. Inst. Meth. A **506** (2003) 250-303

[9] *D. A. Dahl*, SIMION for the personal computer in reflection, Int. J. Mass Spectrom. **200** (2000) 3-25

[10] *W.R. Plass et al.*, The FRS Ion Catcher - A facility for high-precision experiments with stopped projectile and fission fragments, Nucl. Inst. Meth. B **317** (2013) 457-462

[11] *T. Dickel et al.*, A high-performance multiple-reflection time-of-flight mass spectrometer and isobar separator for the research with exotic nuclei, Nucl. Inst. Meth. A **777** (2015) 172-188

[12] *S. Purushothaman et al.*, First experimental results of a cryogenic stopping cell with short-lived, heavy uranium fragments produced at 1000 MeV/u, Eur. Phys. Lett. **104** (2013) 42001

[13] *T. Dickel et al.*, First spatial separation of a heavy ion isomeric beam with a multiple-reflection time-of-flight mass spectrometer, Phys. Lett. B **744**, (2015) 137-141

[14] *R. Kaufmann and R. Wolfgang*, Nucleon Transfer Reactions in Grazing Collisions of Heavy Ions, Phys. Rev. **121** (1961) 192

[15] *J.Galin et.al.*, Mechanism of single-nucleon and multi-nucleon transfer reactions in grazing collisions of heavy ions on silver, Nucl.Phys. A **159** (1970) 461-480

[16] *A. Winther*, Grazing reactions in collisions between heavy nuclei, Nucl.Phys. A **572** (1994) 191-235

[17] *L. Corradi et.al.*, Multinucleon transfer processes in $^{64}Ni +^{238} U$, Phys. Rev. C **59** (1999) 261-268

[18] *A.V. Karpov, V.V. Saiko*, Modeling near-barrier collisions of heavy ions based on a Langevin-type approach, Phys. Rev. C **96** (2017) 024618